

Cite this: *Chem. Sci.*, 2024, 15, 20433

All publication charges for this article have been paid for by the Royal Society of Chemistry

Received 4th October 2024  
Accepted 12th November 2024

DOI: 10.1039/d4sc06723a

rsc.li/chemical-science

# Photocatalytic 1,3-oxyheteroarylation of aryl cyclopropanes with azine *N*-oxides†

Doyoung Kim,<sup>ab</sup> Hyewon Ju,<sup>ab</sup> Wooseok Lee<sup>ab</sup> and Sungwoo Hong<sup>ab\*</sup>

Cyclopropanes, valuable C3 building blocks in organic synthesis, possess high strain energy and inherent stability. We present an efficient, environmentally benign 1,3-oxyheteroarylation of aryl cyclopropanes using azine *N*-oxides as bifunctional reagents under visible light irradiation. This metal-free method yields  $\beta$ -pyridyl ketones under mild conditions. Mechanistic studies reveal a photo-induced radical pathway involving single-electron oxidation of both aryl cyclopropanes and azine *N*-oxides, followed by stepwise ring opening. The dual oxidation mechanism accommodates diverse cyclopropane and azine *N*-oxide combinations based on their oxidation potentials. This green chemistry method enhances the synthetic utility of aryl cyclopropanes while introducing an efficient strategy for their difunctionalization. The methodology aligns with sustainable organic synthesis principles, offering an environmentally conscious route to valuable synthetic intermediates.

## Introduction

Cyclopropane, with its high strain energy and bench stability,<sup>1</sup> has been a versatile component in organic synthesis for decades.<sup>2</sup> Extensive research has focused on utilizing cyclopropane as a C3 building block to develop new skeletal structures through ring-opening/1,3-difunctionalization reactions. These studies have evolved from traditional strategies, such as activating cyclopropane's C–C bond *via* Lewis acid or transition metal coordination, to more recent approaches.<sup>3</sup> Recent advances in photochemistry have opened up promising avenues for creating new reactivity,<sup>4</sup> including the induction of C–C bond cleavage.<sup>5</sup> Notably, several studies have successfully demonstrated the ring-opening of electronically unbiased aryl cyclopropanes through single-electron oxidation under visible light.<sup>6</sup> In this approach, electron-rich cyclopropyl arenes are oxidized by excited photocatalysts, forming aryl cyclopropane radical cations. These reactive species can undergo nucleophilic addition,<sup>7</sup> facilitating attack on the weakened C–C bond and enabling ring opening and functionalization under environmentally friendly conditions.

Despite this significant advance, important limitations remain. The approach is currently restricted to electron-rich aryl cyclopropanes, as electron-deficient variants are inadequately oxidized by the photocatalyst.<sup>6g,8a,c,d</sup> Moreover, the scope of

functional groups capable of reacting with the benzylic radical intermediate has been restricted, typically resulting in products with hydrogen or oxygen substituents at the benzylic position and C–C bond formations are rarely reported.<sup>8</sup> Notably, the incorporation of heteroaryl groups at benzylic radicals generated by such ring-opening reactions has not been reported,<sup>8d</sup> presenting an opportunity to expand the synthetic utility of aryl cyclopropanes in photocatalytic processes (Fig. 1a).

To address these challenges, we envisioned a strategy utilizing the direct oxidation of azine *N*-oxides by an excited-state photocatalyst to generate O-centered radicals.<sup>9</sup> We hypothesized that these O-radicals could enable a previously inaccessible 1,3-functionalization with a broader range of aryl cyclopropanes, including electron-deficient variants. Herein, we present an efficient and environmentally benign method for the 1,3-oxyheteroarylation of various aryl cyclopropanes utilizing azine *N*-oxides as bifunctional reagents under visible light irradiation. Our approach leverages the ability of both aryl cyclopropanes and azine *N*-oxides to undergo photo-induced single-electron oxidation, generating their respective radical cations (Fig. 1b). The reaction proceeds based on the oxidation potentials of the substrates, allowing for a wide range of applications.<sup>8c,9c,d</sup> This method yields  $\beta$ -heteroaryl ketones, offering an efficient strategy for functionalizing these valuable building blocks. Our approach operates under mild conditions, utilizing visible light and azine *N*-oxides as bifunctional reagents, eliminating the need for harsh reagents or toxic metal catalysts. This method enhances the utility of aryl cyclopropanes as synthons for  $\beta$ -heteroaryl ketones, providing an efficient route to important building blocks and valuable synthetic intermediates.

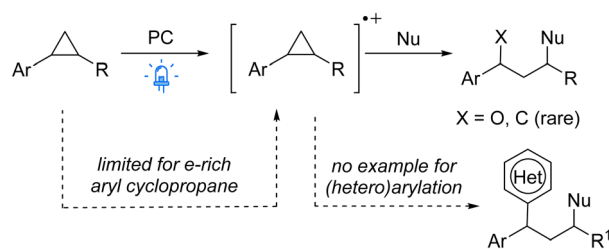
<sup>a</sup>Department of Chemistry, Korea Advanced Institute of Science and Technology (KAIST), Daejeon, 34141, Korea. E-mail: hongorg@kaist.ac.kr

<sup>b</sup>Center for Catalytic Hydrocarbon Functionalizations, Institute for Basic Science (IBS), Daejeon 34141, Korea

† Electronic supplementary information (ESI) available: Experimental procedure, characterization of new compounds (<sup>1</sup>H and <sup>13</sup>C NMR spectra). See DOI: <https://doi.org/10.1039/d4sc06723a>



## a) Visible-light induced 1,3-difunctionalization of arylcyclopropane



## b) This work: 1,3-Oxyheteroarylation via single electron oxidation

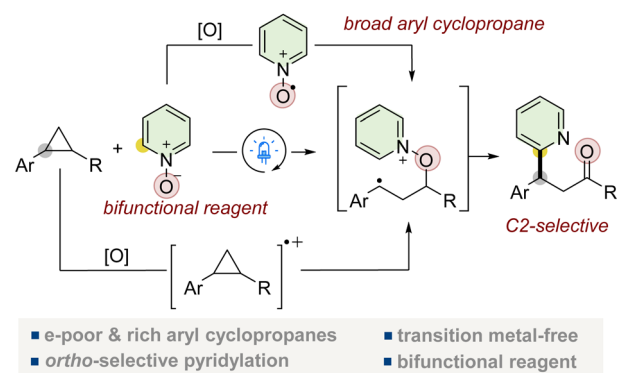


Fig. 1 Overview of photoredox-catalyzed 1,3-functionalization of aryl cyclopropanes. (a) Limitations of previous approaches. (b) This work.

## Results and discussion

We evaluated pyridine *N*-oxide's efficacy as a nucleophile for aryl cyclopropane ring opening using 1,2-diphenylcyclopropane (**1a**) and 2-phenylpyridine *N*-oxide (**2a**) as model substrates under visible light irradiation with a photocatalyst (Table 1). Optimal conditions were identified: 9-mesityl-10-methylacridinium perchlorate (**PC-1**) as photocatalyst and 1-fluoro-2,4,6-trimethylpyridinium triflate (**Py-F**) as oxidant in acetonitrile under blue light, yielding 79% of the 1,3-oxyheteroarylated product (entry 1). Bond formation preferentially occurred at the C6 position of the pyridine core over the C4 position. Alternative oxidants like <sup>t</sup>BuOOH and (PhS)<sub>2</sub> reduced yields (entry 2). Additionally, during our systematic oxidant screening studies, we consistently observed the formation of alcohol as a side product (up to 15% yield). When using **Py-F**, less than 5% of this byproduct is generated in trace amounts (Table S1†). Iridium catalyst **PC-2** gave comparable yields, while **PC-3** showed poor reactivity (entry 3). Moderately polar solvents such as acetone performed well, but polar aprotic solvent (DMSO), nonpolar aprotic solvent (pentane) inhibited the reaction (entry 4). The reaction tolerated water and air, achieving 66% and 56% yields respectively (entry 5). Using O<sub>2</sub> from ambient air as the oxidant led to modest product formation, while the reaction was completely suppressed under pure oxygen atmosphere, suggesting that excessive oxygen may deactivate the photocatalytic cycle through quenching processes (entry 6, Table S5†). Control experiment indicate that the both the photocatalyst and light are essential for the reaction (entry 7).

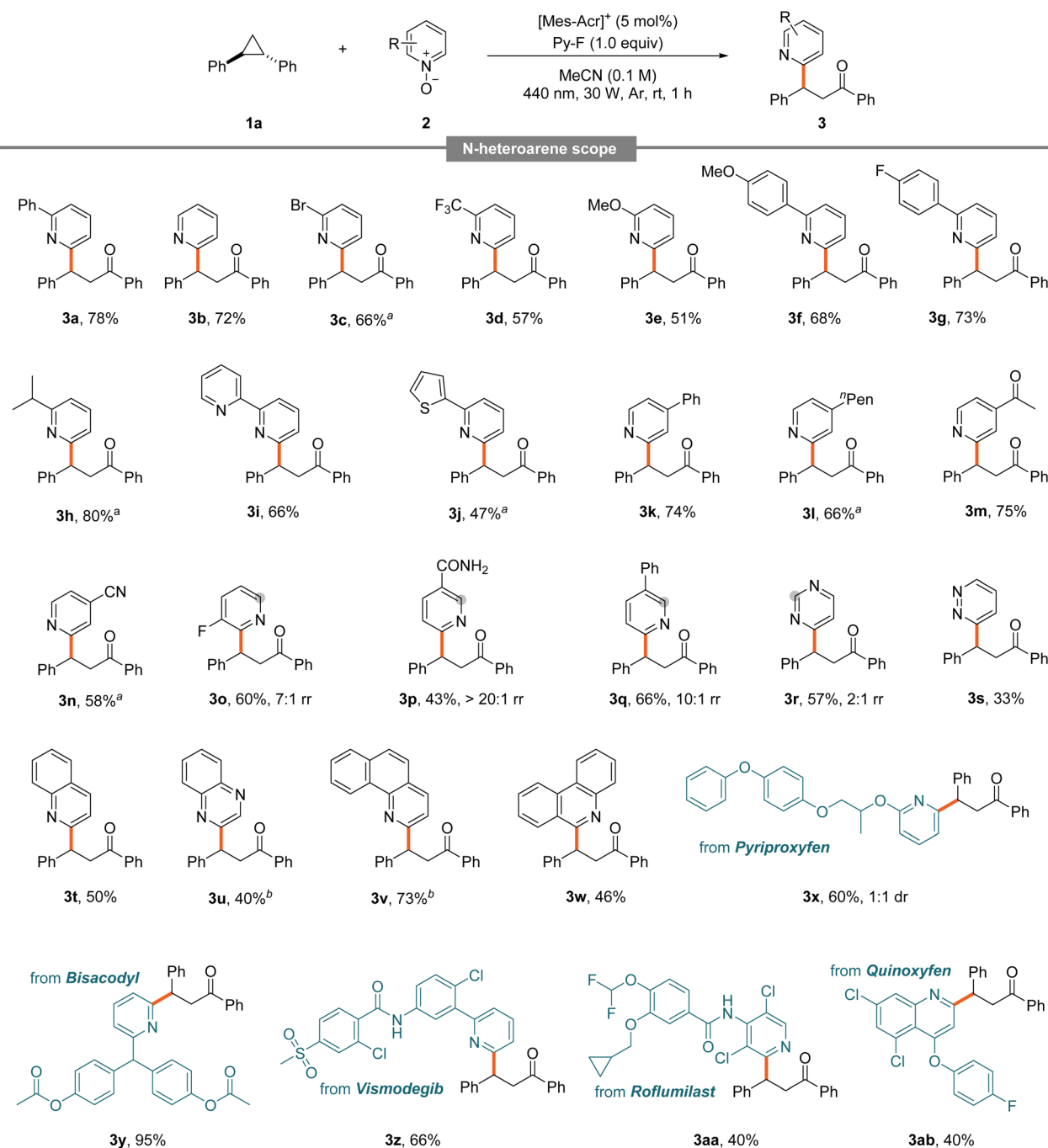
Table 1 Optimization for the reaction conditions<sup>a</sup>

Entry	Variations	Yield <sup>b</sup>
1	None	79% (78%) <sup>c</sup>
2	<sup>t</sup> BuOOH, (PhS) <sub>2</sub> instead of <b>Py-F</b>	55%, 27%
3	<b>PC-2</b> , <b>PC-3</b> instead of <b>PC-1</b>	75%, <sup>d</sup> 7% <sup>d</sup>
4	Acetone, DMSO, <i>n</i> -pentane instead of MeCN	78%, trace, 16%
5	H <sub>2</sub> O (20 μL of), under open air	66%, 56%
6	No <b>Py-F</b> under Ar, air, O <sub>2</sub>	9%, 21%, n.d.
7	No <b>PC</b> , light	Trace

<sup>a</sup> Reaction conditions: **1a** (0.05 mmol), **2a** (1.5 equiv.), **PC** (5 mol%), oxidant (1.0 equiv.) in solvent (0.5 mL) under irradiation with 440 nm LEDs (30 W) at rt for 1 h under argon atmosphere. <sup>b</sup> Yields were determined by <sup>1</sup>H NMR spectroscopy using 1,3,5-trimethoxybenzene as an internal standard. <sup>c</sup> Isolated yield. <sup>d</sup> 2 mol% of **PC** used.

When performed on a larger scale (5.2 mmol), the reaction afforded the desired product in comparable yield. The substrate scope was investigated under optimized conditions. Various azine *N*-oxides afforded 1,3-oxyheteroarylated products (Table 2). Simple pyridine *N*-oxide demonstrated good reactivity (**3b**). 2-Substituted pyridine *N*-oxides performed well with both electron-withdrawing (halogens and CF<sub>3</sub>) and electron-donating (methoxy) groups (**3c–3e**). *N*-Oxides with aryl substituents at the pyridine C2 position showed high efficiency, regardless of electronic properties (**3f** and **3g**). Notably, *N*-oxides with alkyl substituents at the pyridine C2 position exhibited particularly high reactivity (**3h**). Bipyridine, commonly used as a ligand, also provided satisfactory results (**3i**), while moderate conversion was observed with a thiophene-containing substrate (**3j**). Substituted pyridine *N*-oxides with aryl or alkyl groups at the C4 position performed well (**3k** and **3l**). Efficient conversions were also achieved with electron-withdrawing groups, demonstrating broad functional group tolerance (**3m** and **3n**). For 3-substituted pyridine *N*-oxides bearing amide (**3p**) or phenyl (**3q**) groups, radical addition preferentially occurs at the C6 position due to significant steric hindrance. In contrast, with 3-fluorine substituted pyridine *N*-oxide (**3o**), electronic effects dominate the regioselectivity, favoring addition at the more electrophilic C2 position. The reaction was successful with various azine *N*-oxides including pyrimidine, pyridazine, quinoline, and quinoxaline (**3r–3u**). For pyrimidine *N*-oxide, bond formation



Table 2 Azine *N*-oxide scope<sup>a</sup>

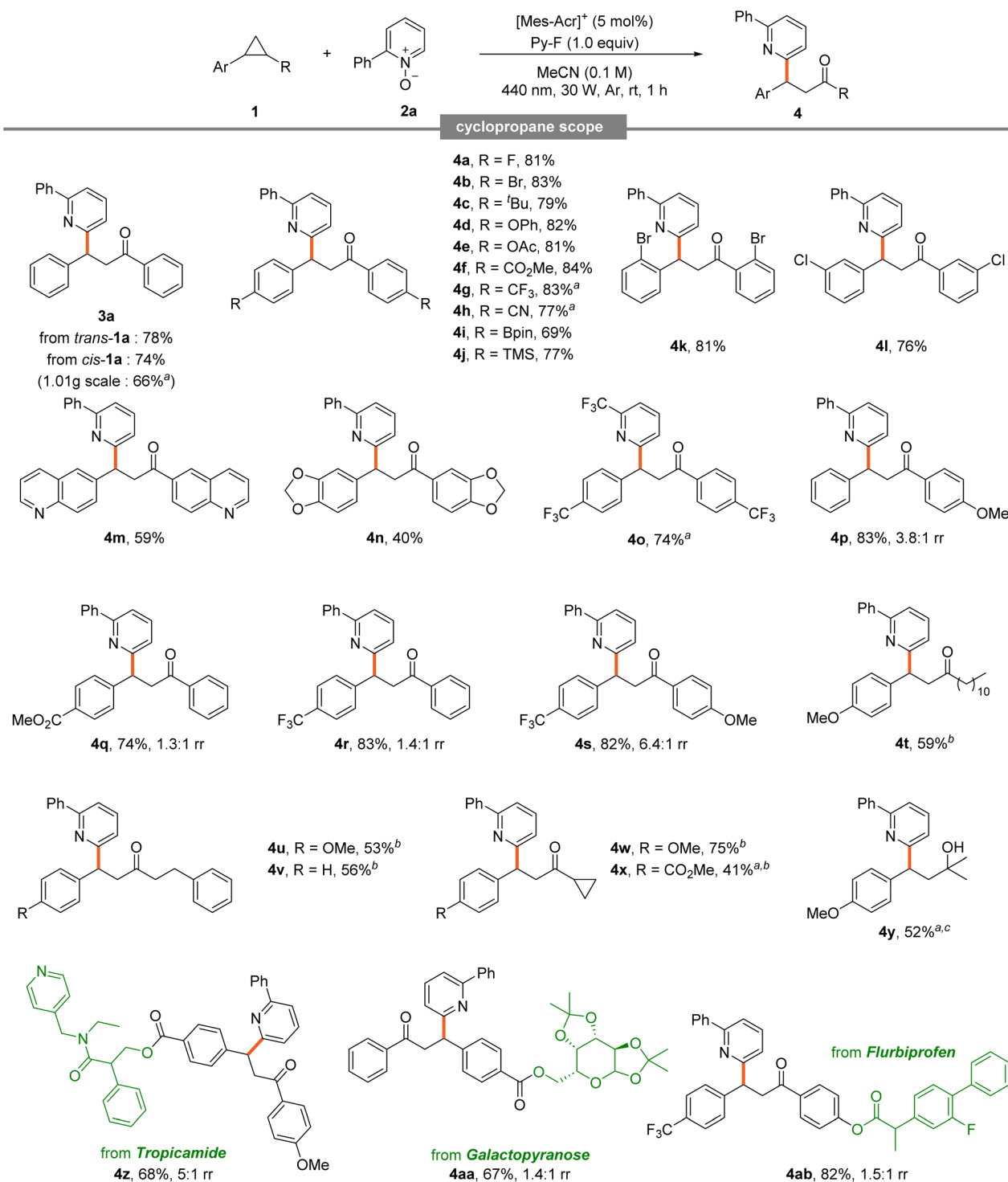
<sup>a</sup> Reaction conditions: **1a** (0.05 mmol), **2** (1.5 equiv.), [Mes-Acr]<sup>+</sup> (5 mol%), Py-F (1.0 equiv.) in MeCN (0.5 mL) under irradiation with 440 nm LEDs (30 W) at room temperature for 1 h under argon atmosphere. Regioisomeric ratios were measured by <sup>1</sup>H NMR spectroscopy. Isolated yield. <sup>a</sup> 3 h for reaction time. <sup>b</sup> 18 h for reaction time.

favoured the C4 position (**3r**). *N*-Oxides containing three rings, such as phenanthridine (a DNA intercalating agent), also demonstrated good efficiency (**3v** and **3w**). Late-stage functionalization was performed on several biorelevant azine *N*-oxides. Derivatives of pyriproxyfen and vismodegib showed good reactivity (**3x** and **3z**), with excellent conversion obtained from

bisacodyl-derived *N*-oxide (**3y**). Quinoxifen and roflumilast derivatives also performed well (**3aa** and **3ab**).

A broad substrate scope was obtained from various cyclopropanes (Table 3). Diphenyl cyclopropane **1a** exhibited excellent reactivity in both *cis* and *trans* forms, even at large scale (**3a**). Symmetric diaryl cyclopropanes generally showed good



Table 3 Cyclopropane scope<sup>a</sup>

<sup>a</sup> Reaction conditions: **1** (0.05 mmol), **2a** (1.5 equiv.), [Mes-Acr]<sup>+</sup> (5 mol%), Py-F (1.0 equiv.) in MeCN (0.5 mL) under irradiation with 440 nm LEDs (30 W) at room temperature for 1 h under argon atmosphere. Regioisomeric ratios were measured by <sup>1</sup>H NMR spectroscopy. Isolated yield. <sup>a</sup> 3 h for reaction time. <sup>b</sup> PC-2 (2 mol%), acetone (0.5 mL) were used. <sup>c</sup> PC-3 (2 mol%), (4-OMePhS)<sub>2</sub> (50 mol%), DCM (0.5 mL) were used.

efficiency. Notably high conversions were observed for those with halogens at the *para* position (**4a** and **4b**). Substrates bearing bulky *t*-butyl groups and electron-rich phenoxy and

acetyl groups exhibited excellent reactivity (**4c–4e**). Notably, good conversions were also achieved with electron-withdrawing groups such as ester, trifluoromethyl, and cyano suggesting



limited electronic influence at the *para* position (**4f–4h**). This clearly demonstrates that the reaction proceeds successfully even in electron-deficient cyclopropanes, where oxidation was previously ineffective in existing studies.

Symmetric diaryl cyclopropanes with *ortho* and *meta* halogen substitutions underwent efficient reactions (**4k** and **4l**). Cyclopropanes containing Bpin and aryl silane, common coupling partners, performed well (**4i** and **4j**). Those with quinoline and piperonyl moieties, frequently observed in biomolecules, also reacted well, demonstrating tolerance to diverse chemical moieties (**4m** and **4n**). Efficient conversion was achieved with CF<sub>3</sub>-substituted pyridine *N*-oxide and an electron-deficient, trifluoromethyl-substituted diaryl cyclopropane (**4o**). Notably, substrates like this trifluoromethyl-substituted diaryl cyclopropane typically possess higher oxidation potentials, making them resistant to oxidation.

The successful transformation of such a challenging substrate underscores the robustness of this method. Unsymmetric diaryl cyclopropanes showed good reactivity, with excellent conversions observed for phenyl rings substituted with methoxy, ester, or trifluoromethyl groups (**4p–4s**). When electron-donating and electron-withdrawing groups were on different rings, good efficiency and improved regioselectivity were observed, indicating that the electronic difference between the two rings can influence the regioselectivity of the reaction.<sup>6d</sup> The substrate scope extended to unsymmetric aryl alkyl

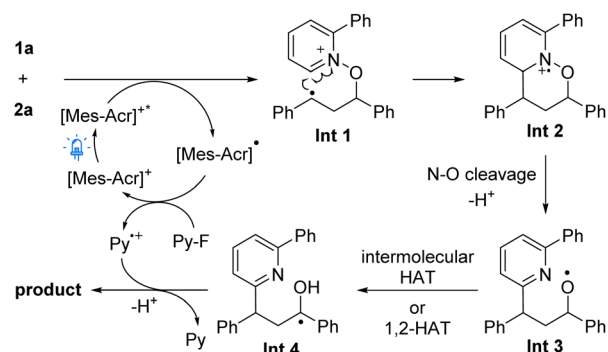


Fig. 3 Proposed reaction mechanism.

cyclopropanes. Alkyl substituents containing undecyl, homobenzyl, and cyclopropyl showed good conversion (**4t–4x**). For molecules with two cyclopropyl rings, ring-opening occurred selectively at the aryl-substituted ring. Dimethyl-substituted cyclopropane, which cannot form a ketone, yielded alcohol as the product (**4y**). Late-stage functionalization of biorelevant cyclopropanes derived from tropicamide, galactopyranose, and flurbiprofen showed good conversions (**4z–4ab**).

To elucidate the reaction mechanism, a series of experiments were conducted. Control experiments ruled out a two-electron pathway involving nucleophilic addition by the *N*-

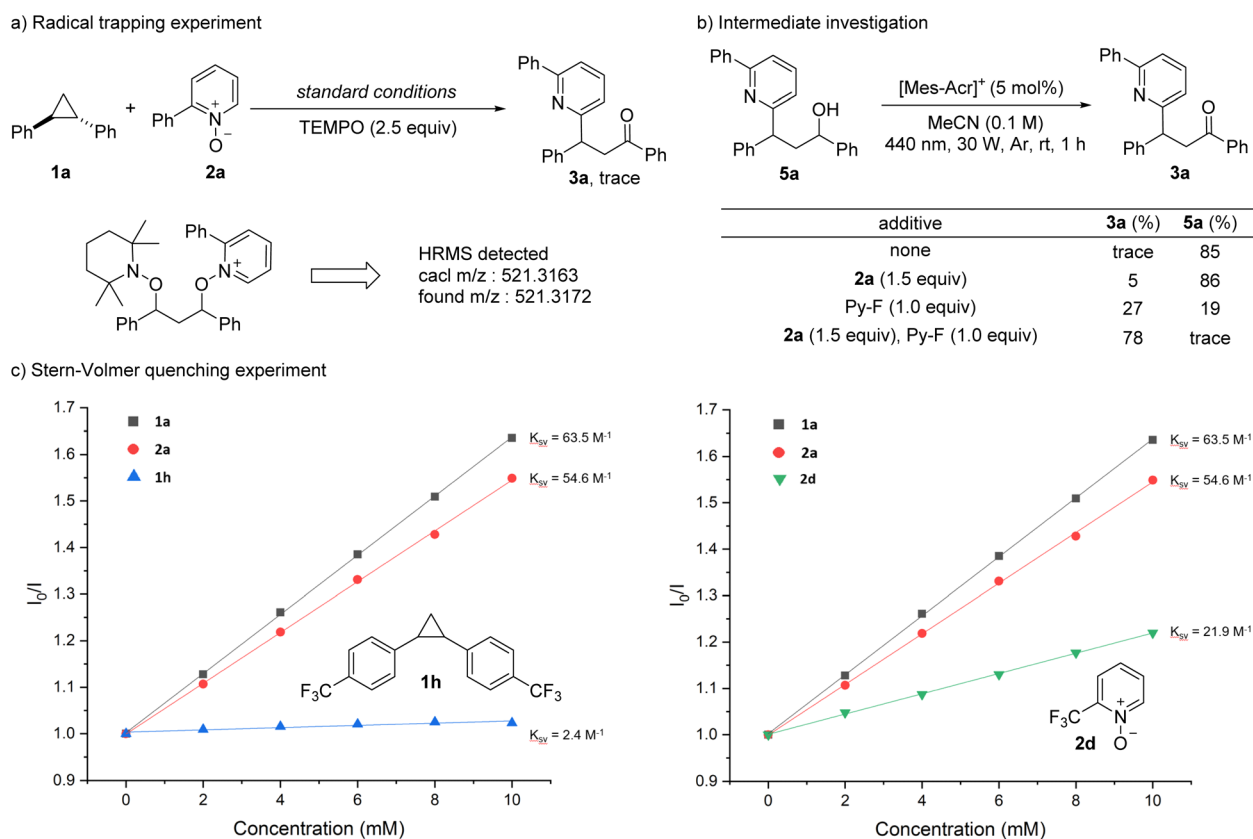


Fig. 2 Control experiments and mechanistic studies. (a) Radical trapping experiments with TEMPO. (b) Oxidation of the alcohol intermediate to ketone. (c) Stern–Volmer quenching experiments.



oxide (Table 1, entry 7). The reaction was inhibited by the radical trapping agent TEMPO, with HRMS detection of a TEMPO adduct confirming a radical pathway (Fig. 2a). Light on-off experiments revealed no additional product formation in the absence of light, suggesting that a radical chain mechanism is unlikely to be operative in this system (Fig. S5†). To investigate the potential oxidation of the *in situ* generated alcohol intermediate to a ketone, we explored various reaction conditions (Fig. 2b). Our experiments revealed that with only the photocatalyst present, ketone conversion was minimal. Similarly, in the presence of pyridine *N*-oxide **2a** alone, the conversion remained minimal and correlated with the amount of photocatalyst used. Notably, without the photocatalyst, no conversion occurred. Interestingly, when Py-F was introduced to the reaction, we observed a 27% yield of **3a**, accompanied by a significant reduction in the alcohol intermediate. Under our standard conditions, which included Py-F, **3a** was produced with a 78% yield, and the alcohol **5a** was almost entirely consumed. These observations suggest that the alcohol compound may function as an intermediate in the reaction pathway. The necessity of both the photocatalyst cycle and *N*-oxide for effective conversion indicates that *N*-oxide plays a crucial role in the oxidation of alcohol to the ketone product. Stern–Volmer quenching experiments identified which substrate undergoes radical initiation upon light exposure. Cyclic voltammetry was then employed to determine the oxidation potentials of the substrates (Fig. 2c and S16–S19†). Both **1a** and **2a** were found to quench the photocatalyst. Subsequent quenching measurements involving electron-deficient cyclopropane and *N*-oxide revealed ineffective photocatalyst quenching. However, successful synthesis of products from combinations such as **1a** with **2d** and **1h** with **2a** suggests two concurrent pathways: (1) ring opening through an S<sub>N</sub>2 reaction of the pyridine *N*-oxide with the cyclopropane radical cation formed by cyclopropane oxidation, and (2) ring opening through an S<sub>H</sub>2 reaction involving the O-centered radical generated by pyridine *N*-oxide oxidation.

Based on the experimental results and previous literature,<sup>6,8</sup> we propose two distinct mechanisms (Fig. 3). Initially, photoexcitation of the photocatalyst facilitates single-electron oxidation of either the cyclopropane or the pyridine *N*-oxide. Nucleophilic attack by the pyridine *N*-oxide **2a** on the oxidized cyclopropane intermediate or the O-centered radical of *N*-oxide to cyclopropane results in cleavage of the C–C bond, forming intermediate **Int 1**. The common pathway proceeds with the benzylic radical in **Int 1** adding to the C-6 position of the pyridine ring, leading to cyclization and formation of **Int 2**.<sup>9a,10</sup> Subsequent N–O bond cleavage and rearomatization produce **Int 3**, which undergoes intermolecular HAT or 1,2-HAT to form **Int 4**.<sup>11</sup> Finally, oxidation of the benzylic radical by the pyridine radical cation yields a benzylic cation, which forms the ketone product **3a** through further deprotonation. In an alternative mechanism, the formation of **Int 3** proceeds as before (Fig. S20 in the ESI†). However, instead of undergoing 1,2-HAT, **Int 3** is reduced by the PC radical, resulting in the formation of the alcohol intermediate. Concurrently, from the second PC cycle, the O-centered radical *N*-oxide is regenerated. This radical acts

as an HAT catalyst, facilitating the conversion of alcohol to **Int 4**. Finally, **Int 4** is oxidized to yield the ketone product **3a**.

## Conclusions

In summary, we have successfully demonstrated the visible light-mediated ring opening of aryl cyclopropanes, yielding 1,3-oxyheteroarylated products. This method offers several significant advantages, including the functionalization of aryl cyclopropanes under mild conditions and broad tolerance for diverse functional groups. The sustainability of this approach is enhanced by the use of readily accessible azine *N*-oxides, which function as efficient bifunctional reagents. Mechanistic studies reveal that both aryl cyclopropane and azine *N*-oxides can quench the photocatalyst through distinct pathways, confirming the involvement of radical processes in this reaction. This efficient approach not only expands the synthetic utility of aryl cyclopropanes but also aligns with the principles of green chemistry, offering a sustainable pathway for the synthesis of complex molecular scaffolds. The method's efficiency, mild conditions, and use of visible light as an environmentally benign energy source represent a significant advancement in sustainable organic synthesis.

## Data availability

The data supporting this article have been included as part of the ESI.†

## Author contributions

D. K., H. J., W. L. performed the experiments, analyzed the data, and wrote the manuscript. S. H. directed the project and wrote the manuscript.

## Conflicts of interest

There are no conflicts to declare.

## Acknowledgements

This research was supported financially by Institute for Basic Science (IBS-R010-A2).

## Notes and references

- (a) A. de Meijere, *Angew. Chem., Int. Ed.*, 1979, **18**, 809–826; (b) K. B. Wiberg, *Angew. Chem., Int. Ed.*, 1986, **25**, 312–322.
- (a) C. Ebner and E. M. Carreira, *Chem. Rev.*, 2017, **117**, 11651–11679; (b) H. N. C. Wong, M. Y. Hon, C. W. Tse, Y. C. Yip, J. Tanko and T. Hudlicky, *Chem. Rev.*, 1989, **89**, 165–198; (c) H.-U. Reissig and R. Zimmer, *Chem. Rev.*, 2003, **103**, 1151–1196.
- (a) T. F. Schneider, J. Kaschel and D. B. Werz, *Angew. Chem., Int. Ed.*, 2014, **53**, 5504–5523; (b) M. A. Cavitt, L. H. Phun and S. France, *Chem. Soc. Rev.*, 2014, **43**, 804–818; (c) H. K. Grover, M. R. Emmett and M. A. Kerr, *Org. Biomol. Chem.*, 2015, **13**,



- 655–671; (d) E. Budynina, K. Ivanov, I. Sorokin and M. Melnikov, *Synthesis*, 2017, **49**, 3035–3068; (e) F. Doraghi, S. Karimian, O. H. Qareaghaj, M. J. Karimi, B. Larijani and M. Mahdavi, *J. Organomet. Chem.*, 2024, **1005**, 122963; (f) K. Ghosh and S. Das, *Org. Biomol. Chem.*, 2021, **19**, 965–982; (g) G. Fumagalli, S. Stanton and J. F. Bower, *Chem. Rev.*, 2017, **117**, 9404–9432; (h) A. S. Adhikari and N. Majumdar, *Eur. J. Org. Chem.*, 2024, **27**, e202301225; (i) E. Budynina, K. Ivanov, I. Sorokin and M. Melnikov, *Synthesis*, 2017, **49**, 3035–3068; (j) A. Ratzenböck, M. Kobras, A. Rustler and O. Reiser, *Chem.–Eur. J.*, 2024, **30**, e202401332.
- 4 (a) R. Liu, S. P. M. Chia, Y. Y. Goh, H. W. Cheo, B. Fan, R. Li, R. Zhou and J. Wu, *Eur. J. Org. Chem.*, 2020, 1459–1465; (b) F. Rammal, D. Gao, S. Boujnah, A. Gaumont, A. A. Hussein and S. Lakhdar, *Org. Lett.*, 2020, **22**, 7671–7675; (c) F. Yuan, D.-M. Yan, P.-P. Gao, D.-Q. Shi, W.-J. Xiao and J.-R. Chen, *ChemCatChem*, 2021, **13**, 543–547; (d) A. Tlili and S. Lakhdar, *Angew. Chem., Int. Ed.*, 2021, **60**, 19526–19549; (e) M. Nakagawa, K. Nagao, Z. Ikeda, M. Reynolds, I. Ibáñez, J. Wang, N. Tokunaga, Y. Sasaki and H. Ohmiya, *ChemCatChem*, 2021, **13**, 3930–3933; (f) U. Karmakar, H. S. Hwang, Y. Lee and E. J. Cho, *Org. Lett.*, 2022, **24**, 6137–6141; (g) C. Hyeon Ka, D. Seul Lee and E. J. Cho, *ChemPhotoChem*, 2022, **6**, e202200136; (h) S. Pan, M. T. Passia, X. Wang, P. Wu, D. Ma and C. Bolm, *Adv. Synth. Catal.*, 2023, **365**, 31–36.
- 5 (a) C. Wang, X. Ren, H. Xie and Z. Lu, *Chem.–Eur. J.*, 2015, **21**, 9676–9680; (b) Ł. Woźniak, G. Magagnano and P. Melchiorre, *Angew. Chem., Int. Ed.*, 2018, **57**, 1068–1072; (c) D. Stavness, T. M. Sodano, K. Li, E. A. Burnham, K. D. Jackson and C. R. J. Stephenson, *Chem*, 2019, **5**, 215–226; (d) M.-M. Wang, T. V. T. Nguyen and J. Waser, *Chem. Soc. Rev.*, 2022, **51**, 7344–7357; (e) Y. Tong, N. Hao, L. Zhang, J. Wei, Z. Zhang, Q. Fu, D. Yi, Y. Mou, J. Wang, X. Pan, L. Yang, S. Wei, L. Zhong and J. Lu, *Org. Chem. Front.*, 2022, **9**, 2129–2134; (f) M. Vellakkaran, T. Kim and S. Hong, *Angew. Chem., Int. Ed.*, 2022, **61**, e202113658; (g) M. Ji, Z. Wu and C. Zhu, *Chem. Commun.*, 2019, **55**, 2368–2371; (h) T. Feng, C. Liu, Z. Wu, X. Wu and C. Zhu, *Chem. Sci.*, 2022, **13**, 2669–2673; (i) Q.-Q. Zhao, X.-S. Zhou, S.-H. Xu, Y.-L. Wu, W.-J. Xiao and J.-R. Chen, *Org. Lett.*, 2020, **22**, 2470–2475; (j) S. Budde, F. Goerdeler, J. Floß, P. Kreitmeier, E. F. Hicks, O. Moscovitz, P. H. Seeberger, H. M. L. Davies and O. Reiser, *Org. Chem. Front.*, 2020, **7**, 1789–1795; (k) M. Kumar, S. Verma, V. Mishra, O. Reiser and A. K. Verma, *J. Org. Chem.*, 2022, **87**, 6263–6272.
- 6 (a) L. Ge, D.-X. Wang, R. Xing, D. Ma, P. J. Walsh and C. Feng, *Nat. Commun.*, 2019, **10**, 4367; (b) D. Petzold, P. Singh, F. Almqvist and B. König, *Angew. Chem., Int. Ed.*, 2019, **58**, 8577–8580; (c) H. Liu, Y. Li, D.-X. Wang, M.-M. Sun and C. Feng, *Org. Lett.*, 2020, **22**, 8681–8686; (d) L. Ge, C. Zhang, C. Pan, D.-X. Wang, D.-Y. Liu, Z.-Q. Li, P. Shen, L. Tian and C. Feng, *Nat. Commun.*, 2022, **13**, 5938; (e) X. Qiao, Y. Lin, D. Huang, H. Ji, C. Chen, W. Ma and J. Zhao, *J. Org. Chem.*, 2022, **87**, 13627–13642; (f) T. V. T. Nguyen, M. D. Wodrich and J. Waser, *Chem. Sci.*, 2022, **13**, 12831–12839; (g) C. Pan, Y. Xu, B. Zhang, L. Ge, C. Zhang and C. Feng, *Cell Rep. Phys. Sci.*, 2023, **4**, 101233.
- 7 (a) J. P. Dinnocenzo, T. R. Simpson, H. Zuillhof, W. P. Todd and T. Heinrich, *J. Am. Chem. Soc.*, 1997, **119**, 987–993; (b) J. P. Dinnocenzo, H. Zuillhof, D. R. Lieberman, T. R. Simpson and M. W. McKechney, *J. Am. Chem. Soc.*, 1997, **119**, 994–1004.
- 8 (a) Z. Zuo, C. G. Daniliuc and A. Studer, *Angew. Chem., Int. Ed.*, 2021, **60**, 25252–25257; (b) Z. Zuo and A. Studer, *Org. Lett.*, 2022, **24**, 949–954; (c) Y. Xu, H.-X. Gao, C. Pan, Y. Shi, C. Zhang, G. Huang and C. Feng, *Angew. Chem., Int. Ed.*, 2023, **62**, e202310671; (d) D. J. Li, X. L. Liu, Y. Zhao and F. Pan, *Org. Lett.*, 2024, **26**, 8063–8068, this work was published while our paper was in preparation.
- 9 (a) W. Zhou, T. Miura and M. Murakami, *Angew. Chem., Int. Ed.*, 2018, **57**, 5139–5142; (b) J.-H. Xu, W.-B. Wu and J. Wu, *Org. Lett.*, 2019, **21**, 5321–5325; (c) B. Wang, C. Ascenzi Pettenuzzo, J. Singh, G. E. McCabe, L. Clark, R. Young, J. Pu and Y. Deng, *ACS Catal.*, 2022, **12**, 10441–10448; (d) M. Schlegel, S. Qian and D. A. Nicewicz, *ACS Catal.*, 2022, **12**, 10499–10505; (e) C. Ascenzi-Pettenuzzo, J. Nganda and Y. Deng, *ChemCatChem*, 2023, **15**, e202300953; (f) L. Laze, B. Quevedo-Flores, I. Bosque and J. C. Gonzalez-Gomez, *Org. Lett.*, 2023, **25**, 8541–8546; (g) B. Wang, J. Singh and Y. Deng, *Org. Lett.*, 2023, **25**, 9219–9224; (h) C. Ascenzi Pettenuzzo, L. Liu, J. Singh, G. Cuffel and Y. Deng, *ChemRxiv*, 2024, DOI: [10.26434/chemrxiv-2024-b32c5](https://doi.org/10.26434/chemrxiv-2024-b32c5).
- 10 (a) Y. Moon, W. Lee and S. Hong, *J. Am. Chem. Soc.*, 2020, **142**, 12420–12429; (b) H. Im, W. Choi and S. Hong, *Angew. Chem., Int. Ed.*, 2020, **59**, 17511–17516; (c) W. Lee, Y. Koo, H. Jung, S. Chang and S. Hong, *Nat. Chem.*, 2023, **15**, 1091–1099.
- 11 (a) C. Che, Q. Huang, H. Zheng and G. Zhu, *Chem. Sci.*, 2016, **7**, 4134–4139; (b) J. Zhang, D. Liu, S. Liu, Y. Ge, Y. Lan and Y. Chen, *iScience*, 2020, **23**, 100755; (c) L.-J. Zhong, H.-Y. Wang, X.-H. Ouyang, J.-H. Li and D.-L. An, *Chem. Commun.*, 2020, **56**, 8671–8674; (d) Y. Chen, D. Liu and J. Zhang, *Synlett*, 2021, **32**, 356–361.

